4-25-2011

Tuning Lattice Thermal Conductance in Ultra-Scaled Hollow SiNW: Role of Porosity Size, Density and Distribution

Abhijeet Paul
Network for Computational Nanotechnology, Purdue University

Kai Miao
Network for Compuational Nanotechnology, Purdue University

Mathieu Luisier
Network for Computational Nanotechnology, Purdue University

Gerhard Klimeck
Network for Computational Nanotechnology, gekco@purdue.edu

Mater. Res. Soc. Symp. Proc. Vol. 1329 © 2011 Materials Research Society
DOI: 10.1557/opl.2011.1464

Tuning lattice thermal conductance in ultra-scaled hollow SiNW: Role of porosity size, density and distribution

Abhijeet Paul*, Kai Miao, Mathieu Luisier, and Gerhard Klimeck
School of Electrical and Computer Engineering,
Network for Computational Nanotechnology,
Purdue University, West Lafayette, IN, 47907, USA.
Email: abhijeet.rama@gmail.com

ABSTRACT

Porous crystalline Si nanowires (PC-SiNW) represent an attractive solution for enhancing the thermoelectric efficiency (ZT) of SiNWs by reducing the lattice thermal conductance (κ_l). A modified valence force field (MVFF) phonon model along with Landauer's approach is used to analyze the ballistic κ_l in PC-SiNWs. A systematic study focusing on the influence of pore size, density, and distribution on the ballistic κ_l of PC-SiNWs is presented. The model predicts a maximum reduction of ~19%, ~23% and ~30% for 1, 2 and 3 pores, respectively with a constant removal of ~12% of the atoms in all the cases. The model also predicts a higher reduction of the ballistic κ_l as the pore separation increases, in the case of 2, 3 and 4 pores, for the same percentage of atoms removed (~12%) in all the cases. Thus, the presence of a high number of small, well-separated pores suppress κ_l strongly. This reduction in ballistic κ_l, in the coherent limit, is attributed to the reduction of the total number of phonon modes and smaller participation of phonon modes (in κ_l) with increasing number of pores.

(1) INTRODUCTION

Silicon has been the backbone of the semiconductor industry for the last 60 years which has led to the development of very well established fabrication processes. This has resulted into numerous efforts to integrate Si as a viable thermoelectric (TE) material in solid state circuits and devices [1-4]. Bulk Si is a poor TE material (ZT ~0.06 at 300K [1]) however, Si nanowires have shown very promising room temperature thermoelectric efficiency (ZT ~0.6 at 300K) [1]. This significant improvement (~100X higher compared to bulk Si) is attributed to the drastic reduction in lattice thermal conductivity in SiNWs. Some interesting experimental [2-4] and theoretical [5, 6] efforts to further reduce the lattice thermal conductivity in silicon by creating pores in crystalline bulk Si have been reported. The artificial pore creation in crystalline Si can block the phonon transport in crystalline Si, thereby reducing the thermal conductivity as amorphours-Si (am-Si), but PC-SiNW has the advantage that the crystalline nature allows electrons to conduct quite well, thus maintaining a good electrical conductance (G) and Seebeck coefficient (S), needed for higher thermoelectric figure of merit (ZT), unlike am-Si.[5]

Many technological improvements have led to the fabrication of hollow crystalline nanowires. Some of the main fabrication techniques are (i) hollow nanowire array fabrication using sacrificial templates [7], (ii) hollow spinel wires using the `Kirkendall effect' [8], (iii) electrochemical anodic dissolution [9], (iv) template based patterned nanowire fabrication [10] and (v) deep reactive ion etching (DRIE) [4].

Motivated by these experimental progresses in the fabrication of crystalline porous SiNWs, we carried out a systematic study to understand the impact of pores on the ballistic lattice thermal conductance (κ_l) of ultra-scaled SiNWs in the coherent phonon limit. In the present work, we study the impact of (i) pore size, (ii) pore density and (iii) pore distribution on κ_l. This allows us to identify ways to better tune κ_l and hopefully guide the improved fabrication

methods [4, 7-10] to obtain better TE structures made of Si. This work has the following parts. Section 2 provides a brief description of the method used to calculate the phonon dispersion in hollow SiNWs and to obtain the lattice thermal conductance from the phonon spectra. Section 3 shows the results on tuning thermal conductance using pores and discusses the reasons for the reduction in κ_l. Section 4 summarizes the main points of the work.

(2) THEORY AND APPROACH

The ballistic κ_l is calculated using Landauer's approach [11] and the full phonon dispersion of hollow SiNWs. The steps in the analysis procedure are provided below:

1. Atoms are arranged to form a SiNW with specific cross-section size (W/H) and channel orientation. No structure relaxation is performed for the wires which is important for cross-sections W < 1nm [12].
2. Depending on the type and radius of the pore, atoms are removed from the SiNWs (Fig.1). The reomoved atoms are always less than 25% of the total atoms composing the considered unitcell in order to ensure structural stability of the wire (no negative phonon dispersion was obtained [13]).
3. The equation of motion for each atom is assembled into a 'dynamical matrix' using a Modified Valence Force Field (MVFF) potential model [14, 15].
4. The atoms on the outer and inner surfaces are allowed to vibrate freely which enter as the boundary condition into the dynamical matrix [15].
5. The eigen frequencies (ν) and the eigen displacement vectors (φ) are obtained by diagonalizing the dynamical matrix [15].
6. Using ν, the lattice thermal conductance (κ_l) is calculated based on Landauer's approach [11].

A more detailed description of the calculation steps are provided in Ref. [15]. Next, we briefly describe the phonon model, thermal conductance calculation, and details of the SiNWs used in this study.

Phonon Model: The phonon dispersion in free-standing SiNWs is calculated using a Modified Valence Force Field (MVFF) model [14], where the frequencies of all the phonon modes are calculated from the forces acting on atoms produced by finite and periodic displacements of the atoms in a crystal at equilibrium. The MVFF model captures the bulk phonon dispersions (for both relaxed and strained crystals) as well as other lattice properties in bulk Si, Ge, etc. [14, 15] and has been recently applied to SiNWs to explain their phonon spectra and lattice thermal properties [16].

Lattice thermal conductance (κ_l): The thermal conductance of a SiNW with its two leads maintained at temperature T and T+ΔT (where ΔT is very small) is calculated using Landauer's formula [11] as [16, 17],

$$\kappa_l = \frac{1}{h}\int_0^{E_{\max}} P(E)\cdot M(E)\cdot E\cdot \frac{\partial}{\partial T}\left[(\exp(\frac{E}{k_B T})-1)^{-1}\right]\cdot dE, \qquad (1)$$

(1)

where E (= hν, h is Planck's constant) is the phonon energy, M(E) is the number of phonon modes at energy E, P(E) is the transmission of the mode at E, E_{max} is the maximum phonon vibration energy and K_b is Boltzmann's constant. Since the κ_l is calculated in the ballistic limit, P(E) is 1 for all the modes. In the case of diffusive transport P(E) is generally less than 1[17].

Si Nanowire details: In the present study only rectangular SiNWs with [100] wire axis orientation have been considered**.** The width (W) and the height (H) of the SiNWs vary from 3nm to 5nm. The number of pores varies from 1 to 4 (Figure 1). The pore radius (R_h) varies

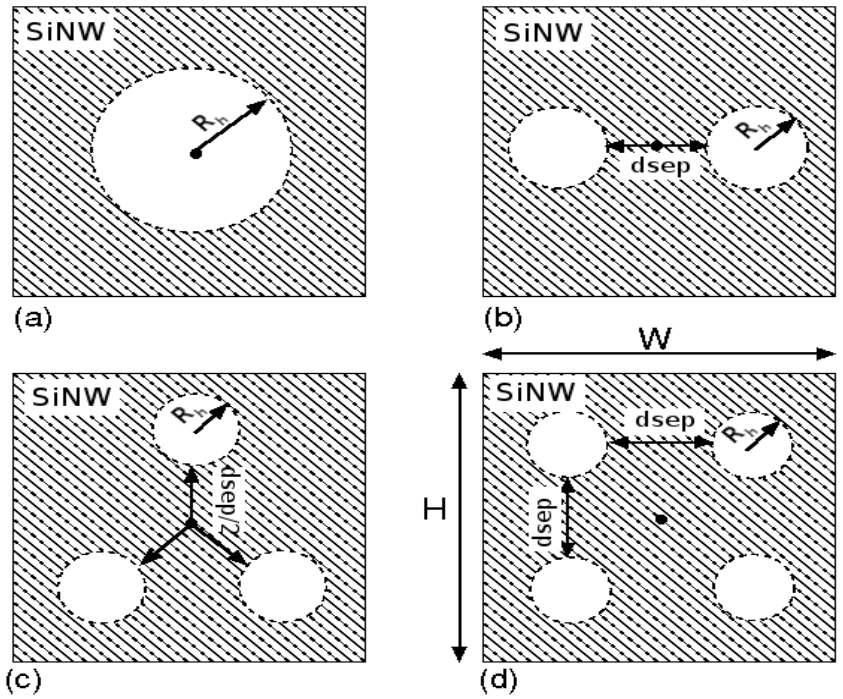

Figure 1: Schematic of SiNWs with different pore density, (a) 1 pore, (b) 2 pores, (c) 3 pores and (d) 4 pores. The width (W) and height (H) of the SiNWs vary between 3nm to 5nm. To understand the impact of pore density on the ballistic thermal conductance (κ_l) a similar percentage of atoms (~12 %) are removed for all the cases (a-d) The separation between the holes (d_{sep}) is also changed from 0 to 1nm in steps of 0.2nm to study the impact of pore distribution on κ_l.

from 0 to 0.8nm. The separation between the pores (d_{sep}) is varied from 0 to 1nm in steps of 0.2nm each. The meaning of d_{sep} for each case is shown in Figure 1. There are multiple ways to create separation among the pores. The idea is to understand the impact of pore separation in an ordered manner. These pores could be generated randomly too (close to experiments), which will affect κ_l, but this is beyond the scope of the present work.

(3) RESULTS AND DISCUSSION

In this section we present the impact of pores on the phonon dispersion and ballistic lattice thermal conductance of SiNWs. We also discuss the reasons for the observed reduction in κ_l.

Phonon dispersion in hollow SiNWs: The presence of pores bring down more phonon bands in the lower energy regime as shown in Fig. 2 a-c. The presence of 3 and 4 pores in a 4nm X 4nm SiNW brings down 14 and 18 sub-bands below 7 meV, (this energy value is chosen arbitrarily) respectively (Fig. 2 a-b). However, a same sized filled (solid) SiNW has only 10 phonon sub-bands below 7meV (Fig. 2c). Higher number of phonon bands in hollow wires contribute more to κ_l in the lower energy regime but soon the filled SiNW shows higher contribution due to the larger number of modes in higher energy section (Fig. 2d-e). The sound velocity in hollow SiNWs is reduced by ~30% (for 3 pore case) compared to filled SiNWs which also affect heat transport. Thus, hollow wires still show an overall reduction in κ_l compared to filled wires.

Reduction in ballistic κ_l : The presence of pores reduces the ballistic lattice thermal conductance even in the absence of scattering processes. The impact of pore size, density and distribution on κ_l is discussed next.

I. Effect of porosity size (R_h): The size of the pore has a direct influence on the thermal conductance. As R_h increases, κ_l drops. For Si NWs with different W/H κ_l reduces as shown in Fig. 3. Wires with smaller cross-section sizes show a larger reduction in κ_l. A 3nm X 3nm SiNW

shows a reduction of ~38% in κ_l for a hole of radius 0.8nm whereas, a 4nm X 5nm SiNW shows ~19% reduction (Fig. 3). Thus, creating pores in smaller cross-section wires can reduce κ_l more drastically compared to larger cross-section size NWs.

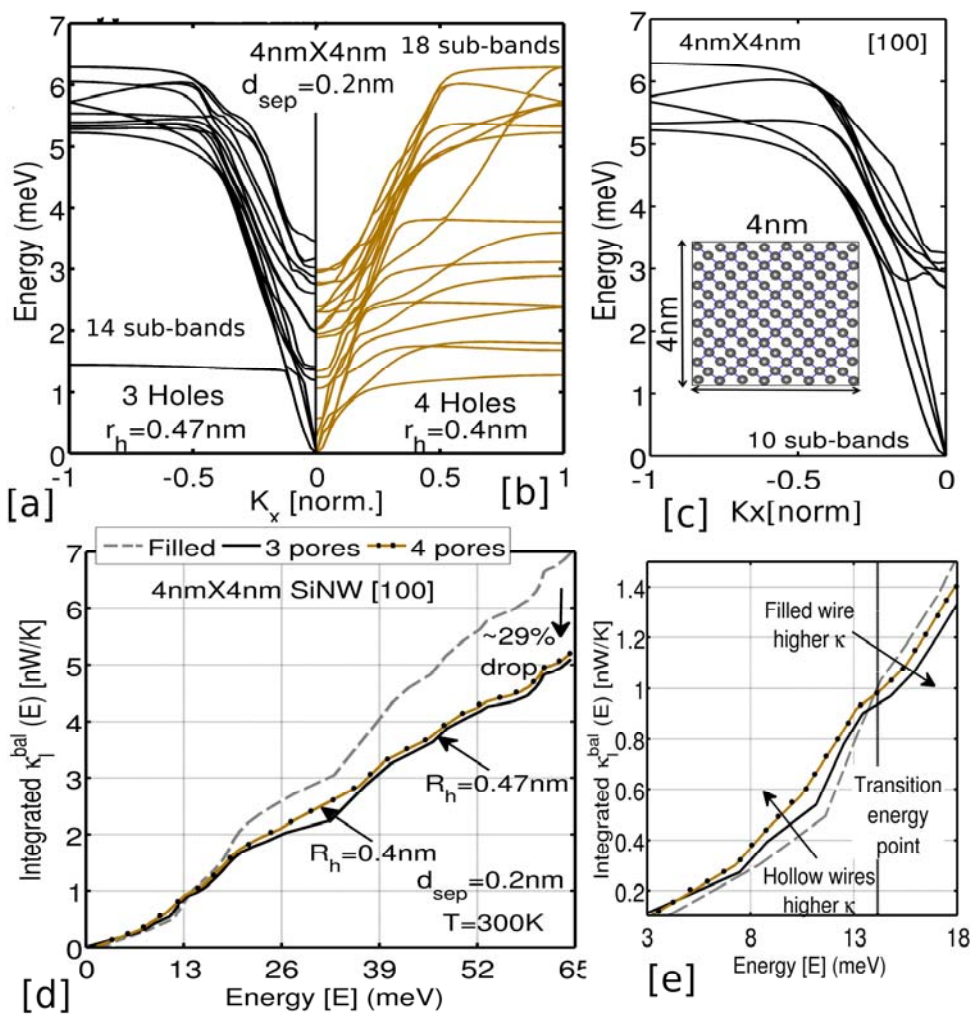

Figure 2: Phonon dispersion for 4nm X 4nm hollow [100] SiNW with (a) 3 pores (R_h=0.47nm) and (b) 4 pores (R_h = 0.4nm) with a separation of 0.2 nm among the pores. (c) Phonon dispersion for 4nm X 4nm filled square SiNW. Inset shows the projected atomic unitcell of the filled SiNW. Only the first 10 sub-bands are below 7meV for the filled SiNW where as 14 and 18 sub-bands are within 7meV for 3 and 4 pores, respectively. (d) Sub-band contribution to the lattice thermal conductance for the three cases at 300K. (e) A closer look at the variation in κ_l for smaller energy range. Intially hollow wires show higher contribution but filled wire overtakes as sub-bands beyond 14meV start contributing.

II. Effect of porosity density and separation: The reduction in κ_l shows a strong dependence on the number of pores in the SiNW. At d_{sep} = 0nm, all the pore cases show very similar reduction in κ_l (~22% -23%) (Fig. 4), which is expected since at dsep = 0nm all the cases coincide with the 1 pore case. As the separation between the pores increases the κ_l reduction shows different results for different pore density. The 2 and 4 pore cases show a reduction of ~22% to ~24% when the pore separation changes from 0nm to 1nm (Fig. 4). However, the 3 pore case shows a much higher reduction from ~24% to ~30% for the same change in pore separation (Fig. 4). This non-monotonic behavior of κ_l reduction with pore density can be explained using phonon localization (discussed later). It turns out that the phonon mode reduction and mode participation reduction is higher for the 3 pores case (Fig. 5b and 6b). Hence, the pore density and their separation can be an effective way for tuning κ_l.

Reasons for the reduction in κ_l:

Creation of pores in SiNWs breaks the crystal symmetry which affects the phonon dispersion and causes a drop in κ_l. In the coherent phonon limit, there are two main reasons responsible for the reduction in κ_l :

I. Reduction in phonon modes (M(E)): The total number of phonon modes has a direct impact on κ_l (Eq. 1). The total number of phonon modes reduces with pore size (Fig. 5a). A ~50% reduction in modes with pore size (Fig. 5a) reduces κ_l by ~38% in a 3nm X 3nm SiNW (Fig.4).

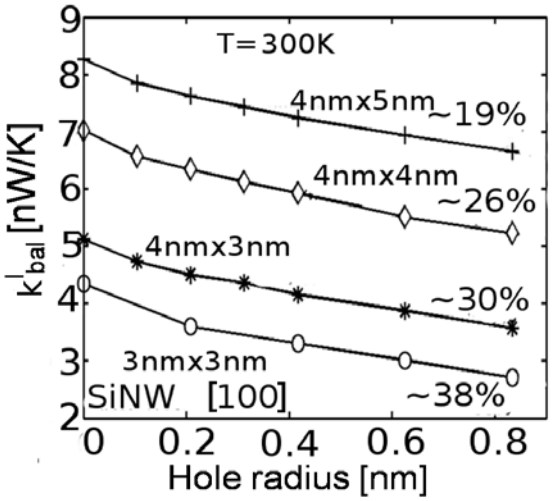

Figure 3: Ballistic κ_l at 300K in small cross-section rectangular [100] SiNWs with different cross-section sizes and pore radius (R_h). The percentage reduction in κ_l for all the SiNWs at R_h = 0.8nm is also indicated.

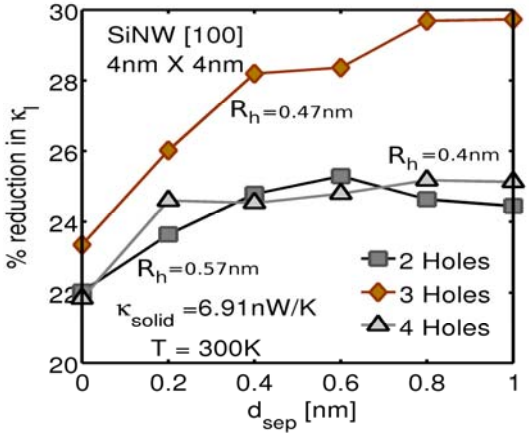

Figure 4: Percentage reduction in κ_l with hole density and their separation (d_{sep}) in a 4nm X 4nm [100] SiNW at 300K. Hole radius for 2 holes, 3 holes and 4 holes case is 0.57nm, 0.47nm and 0.4nm, respectively Aprrox. 12.5% atoms removed in all the cases. The reduction in κ_l increases with the separation in holes and also shows maximum reduction for the 3 holes case.

II. Phonon Participation ratio: Creation of pores reduce the crystal symmetry which does not allow the phonons to propagate properly (or they get localized) [18, 19]. The extent of phonon mode participation can be measured using a number called `participation ratio' (PR) [18, 19]. The participation ratio measures the fraction of atoms participating in a mode and hence varies between O(1) for delocalized states to O(1/N) for localized states and effectively indicates the fraction of atoms participating in a given mode. PR can be calculated for each phonon mode as [19],

$$PR^{-1} = 3N \sum_i \left(\sum_{n,j \in [x,y,z]} \phi_{i,n,j} \cdot \phi^*_{i,n,j} \right)^2, \qquad (2)$$

where N is the total number of atoms in the unit cell and $\varphi_{i,n,j}$ is the eigen vector (step5) associated with atom `i', sub-band `n' and direction `j'.

The PR value decreases with increasing pore size for a 3nm SiNW (Fig. 6a). The PR value reduces more for 3 pores case as the pore separation increases compared to the 2 and 4 pore cases (Fig .6b). This explains the larger reduction in κ_l for 3 pores case (Fig.4) which has a higher phonon localization. This indicates that the 3 pores case breaks the crystal symmetry strongly.

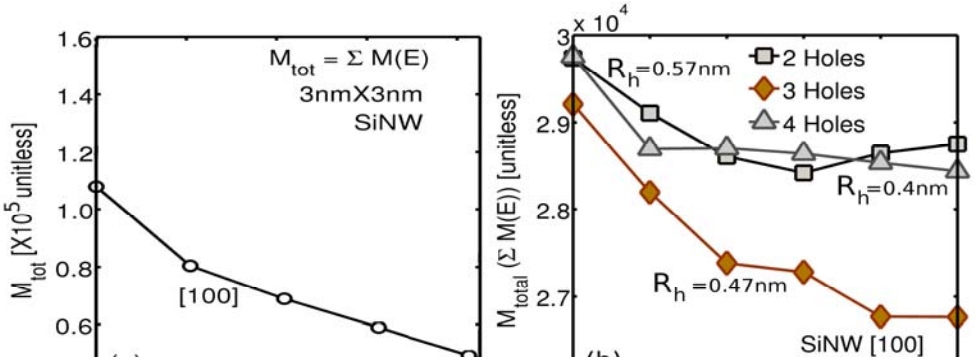

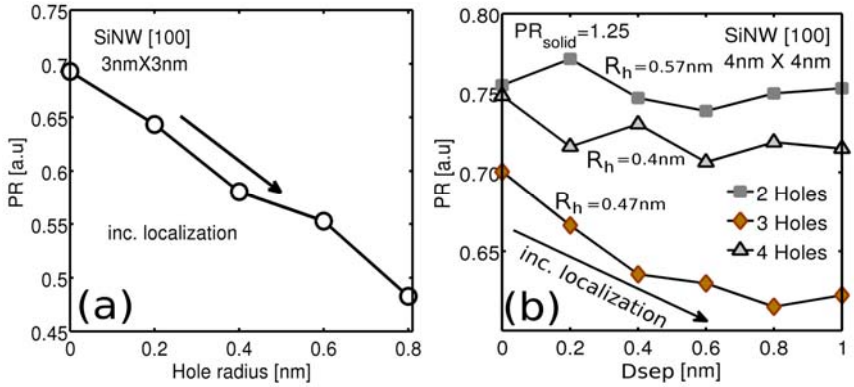

Figure 6: Participation ratio indicating the localization of phonons in SiNWs (a) PR value decreases as pore size increases for 3nm X 3nm SiNW showing higher phonon localization in wires with larger pores. (b) PR value for different types of pores in a 4nm X 4nm size SiNW. 3 pore case shows the maximum phonon localization.

(4) CONCLUSIONS

The presence of pores in SiNWs can be used for tuning their thermal conductance. Increased phonon confinement, phonon localization due to increased surface-to-volume ratio and decrease in phonon modes are the reasons for such drastic reduction in κ_l in the coherent phonon limit. Thus, (a) the variation of nanowire cross-section size, (b) the pore radius, (c) the pore density, and (d) the pore separation, provide technologically viable ways to engineer the lattice thermal conductance. This can pave the way to make better TE devices using Si nanowires.

ACKNOWLEDGMENTS

The authors acknowledge financial support from MSD a Semiconductor Research Corporation (SRC) entity, Nanoelectronics Research Initiative (NRI) through MIND, NSF (GrantNo.OCI -0749140) and Purdue University. Computational support from nanoHUB.org, an NCN operated and NSF (Grant No .EEC-0228390) funded project, is also acknowledged.

REFERENCES

[1] A. I. Hochbaum, R. Chen, R. D. Delgado, W. Liang, E. C. Garnett, M.Najarian, A. Majumdar, and P. Yang, Nature (London) 451, 163, (2008).
[2] G. Gesele, J. Linsmeier, V. Drach, J. Fricke, and R. Arens-Fischer, J. Phys.D: Appl. Phys. 30, 2911 (1997).
[3] J.-K. Yu, S. Mitrovic, D. Tham, J. Varghese, and J. R. Heath, Nat. Nanotechnol. 5, 718 (2010).
[4] P. E. Hopkins, C. M. Reinke, M. F. Su, R. H. Olsson, E. A. Shaner, Z. C. Leseman, J. R. Serrano, L. M. Phinney, and I. El-Kady Nano Lett., 11 (1), pp 107–112,(2011)
[5] J.-H. Lee, G. A. Galli, and J. C. Grossman, Nano Lett. 8, 3750 (2008).
[6] A Paul and G. Klimeck, Appl. Phys. Lett. 98, 083106; doi:10.1063/1.3556648, 3 pages, (2011).
[7] Y. Cao, J. He, and J. Sun, Mater. Lett. 63, 148 (2009).
[8] H. J. Fan, M. Knez, R. Scholz, K. Nielsch, E. Pippel, D. Hesse, M. Zacharias, and U. Gosele, Nature Mater. 5, 627 (2006).
[9] R. Srinivasan, M. Jayachandran, and K. Ramachandran, Cryst. Res. Technol. 42, 266 (2007).
[10] L. C. L. Y. Voon, Y. Zhang, B. Lassen, M. Willatzen, Q. Xiong, and P. C. Eklund, J. Nanosci. Nanotech. 8, 1 (2008).
[11] R. Landauer, IBM J. Res. Dev. 1, 223 (1957).
[12] A. Palaria, G. Klimeck, and A. Strachan, Phys. Rev. B 78, 205315 (2008).
[13] H. Peelaers, B. Partoens, and F. M. Peeters, Nano Lett. 9, 107 (2009).

[14] Z. Sui and I. P. Herman, Phys. Rev. B 48, 17938 1993.
[15] A. Paul, M. Luisier, and G. Klimeck, J. Comput. Electron. 93, 160 (2010).
[16] A. Paul, M. Luisier, and G. Klimeck, 14th Int. Workshop on Comp. Elect.(IWCE), pp. 1–4, 2010.
[17] N. Mingo, L. Yang, D. Li, and A. Majumdar, Nano Lett. 3, 1713 (2003).
[18] J. Chen, G. Zhang, and B. Li, Nano Lett. 10, 3978 (2010).
[19] A. Bodapati, P. K. Schelling, S. R. Phillpot, and P. Keblinski, Phys. Rev. B 74, 245207 (2006).